

UKAEA-CCFE-CP(23)20

A. SABBAGH, J.W. BERKERY, Y.S. PARK, J.H. AHN,
Y. JIANG, J.D. RIQUEZES, J. BUTT, J. BIALEK, J.G.
BAK, M.J. CHOI, S.H. HAHN, J. KIM, J. KO, W.H. KO,
J.W. LEE, J.H. LEE, K.D. LEE, L. TERZOLO, S.W.
YOON, R.E. BELL, M.D. BOYER, et al.

TOKAMAK DISRUPTION EVENT CHARACTERIZATION AND FORECASTING RESEARCH AND EXPANSION TO REAL-TIME APPLICATION

This document is intended for publication in the open literature. It is made available on the understanding that it may not be further circulated and extracts or references may not be published prior to publication of the original when applicable, or without the consent of the UKAEA Publications Officer, Culham Science Centre, Building K1/O/83, Abingdon, Oxfordshire, OX14 3DB, UK.

Enquiries about copyright and reproduction should in the first instance be addressed to the UKAEA Publications Officer, Culham Science Centre, Building K1/O/83 Abingdon, Oxfordshire, OX14 3DB, UK. The United Kingdom Atomic Energy Authority is the copyright holder.

The contents of this document and all other UKAEA Preprints, Reports and Conference Papers are available to view online free at scientific-publications.ukaea.uk/

TOKAMAK DISRUPTION EVENT CHARACTERIZATION AND FORECASTING RESEARCH AND EXPANSION TO REAL-TIME APPLICATION

A. SABBAGH, J.W. BERKERY, Y.S. PARK, J.H. AHN, Y. JIANG,
J.D. RIQUEZES, J. BUTT, J. BIALEK, J.G. BAK, M.J. CHOI, S.H.
HAHN, J. KIM, J. KO, W.H. KO, J.W. LEE, J.H. LEE, K.D. LEE, L.
TERZOLO, S.W. YOON, R.E. BELL, M.D. BOYER, et al.

TOKAMAK DISRUPTION EVENT CHARACTERIZATION AND FORECASTING RESEARCH AND EXPANSION TO REAL-TIME APPLICATION

S.A. SABBAGH, J.W. BERKERY, Y.S. PARK, J.H. AHN, Y. JIANG, J.D. RIQUEZES, J. BUTT, J. BIALEK
Department of Applied Physics and Applied Mathematics, Columbia University
New York, NY, USA
Email: sabbagh@pppl.gov

J.G. BAK, M.J. CHOI, S.H. HAHN, J. KIM, J. KO, W.H. KO, J.W. LEE, J.H. LEE, K.D. LEE, L. TERZOLO, S.W. YOON
Korea Institute of Fusion Energy
Daejeon, Republic of Korea

R.E. BELL, M.D. BOYER, K. ERICKSON, B. LEBLANC, M. PODESTA, Z.R. WANG, J. YOO
Princeton Plasma Physics Laboratory
Princeton, NJ, USA

C. HAM, A. KIRK, L. KOGAN, D. RYAN, A. THORNTON, J. HOLLOCOMBE
Culham Centre for Fusion Energy
Abingdon, UK

F.M. LEVINTON, M.GALLANTE
Nova Photonics
Princeton, NJ, USA

Abstract

Disruption prediction and avoidance is critical for ITER and reactor-scale tokamaks to maintain steady plasma operation and to avoid damage to device components. The present status and results from the disruption event characterization and forecasting (DECAF) research effort are shown. The DECAF paradigm is primarily physics-based and provides quantitative disruption prediction for disruption avoidance. DECAF automatically determines the relation of events leading to disruption and quantifies their appearance to characterize the most probable and deleterious event chains, and to forecast their onset. Automated analysis of rotating MHD modes now allows the identification of disruption event chains for several devices including coupling, bifurcation, locking, and potential triggering by other MHD activity. DECAF can now provide an early disruption forecast (on transport timescales) allowing the potential for disruption avoidance through profile control. Disruption prediction research using DECAF also allows quantifiable figures of merit (i.e. the plasma disruptivity) to provide an objective assessment of the relative performance of different models. There is an extensive physics research effort supporting DECAF model development. First, analysis of high performance KSTAR experiments using TRANSP shows non-inductive current fraction has reached 75%. Resistive stability including Δ' calculation by the Resistive DCON code is evaluated for these plasmas. "Predict-first" TRANSP analysis was performed showing that with the newly-installed 2nd NBI system (assuming usual energy confinement quality and Greenwald density fraction), 100% non-inductive plasmas scenarios are found in the range $\beta_N = 3.5$ –5.0. Second, new analysis of MAST plasmas has uncovered global MHD events at high β_N identified as resistive wall modes (RWMs). A stability analysis of MAST plasmas shows a significant ballooning shape of the three-dimensional RWM eigenfunction that compares well to fast camera images. Real-time DECAF analysis is now being constructed for KSTAR. Four of five real-time (r/t) computers and diagnostic interfaces have been installed to measure and decompose rotating MHD activity, measure the r/t toroidal plasma velocity profile, r/t plasma electron temperature profile, and provide r/t two-dimensional measurement of electron temperature fluctuations at a given toroidal position. A fifth system to provide r/t measurement of the internal magnetic field pitch angle profile using the motional Stark effect is under design for installation in the coming year.

1. INTRODUCTION

Disruption prediction and avoidance is critical for ITER and reactor-scale tokamaks to maintain steady plasma operation and to avoid damage to device components. Effective, practical disruption control approaches need to forecast and avoid disruption providing near-continuous operation of a tokamak with very low disruptivity rates (less than 2% to meet excessive transient electromagnetic forces and first wall thermal loads on ITER). Even lower levels are desired to avoid issues related to runaway electron generation and to provide continuous operation of future energy-producing power plants. Such approaches need to be demonstrated to work across

multiple tokamak devices and be physics-based to best ensure extrapolability to future machines. Results from the Disruption Event Characterization and Forecasting (DECAF) research effort have been shown for multiple tokamak devices [1]. Access to the full KSTAR, MAST, NSTX, AUG, and TCX databases is presently available. Required characteristics of such systems to support both continuous and asynchronous plasma control have been defined by Humphreys, et al. [2] These include the prediction of specific pre-disruptive phenomena linked to plasma control and providing continuous quantitative assessment determining proximity to undesirable operating states (“warning levels”). These warning levels must be calculable in real-time. Such systems must also provide sufficient lead time in disruption forecasting to actuate plasma control to avoid the disruption. They must also be extrapolable to new devices. The DECAF approach to disruption avoidance in tokamaks meets these criteria.

This paper provides an overview of DECAF, statement of present performance, and recent DECAF event development (Section 2). Several physics studies and analyses support DECAF research, including resistive wall mode stability investigation of MAST plasmas and transport and stability analysis of KSTAR plasmas (Section 3) with further detail shown in three other papers at this conference [3,4,5]. The research has most recently put strong focus on implementing five real-time data acquisition systems on the KSTAR device supporting the calculation of DECAF disruption forecast warning levels and events in real time (Section 4).

2. DISRUPTION EVENT CHARACTERIZATION AND FORECASTING

2.1. Overview

The DECAF approach to disruption avoidance is primarily physics-based and provides both a qualitative analysis of the physical events leading to a plasma disruption and quantitative figures of merit determining how well the forecasting system performs. Some examples of the latter include how early a disruption forecast is made compared to when the disruption actually happens, and how accurate the forecasts are (true and false positive rates). The DECAF code was written to automatically determine the relation of events leading to disruption and quantify their appearance to characterize the most probable and deleterious “event chains”, and forecast their onset. The idea of disruption event chains in DECAF largely follows from a manual analysis established by de Vries, et al. [6] for JET. DECAF provides an understanding of the event dynamics leading to disruptions to ensure disruption forecasting extrapolability to ITER and future devices in which the production of disruptions in the device to teach non-physics-based approaches is highly restricted.

A description of the DECAF code, demonstration of DECAF events chains and conclusions based on analysis of the KSTAR, MAST, and NSTX databases are given in Ref. 1. Connection to the ASDEX Upgrade database has now been made. For convenience and to most succinctly understand some key code capabilities, a compilation of results are shown in Fig. 1 below for an NSTX plasma disruption initiated by the onset of a toroidal mode number $n = 1$ rotating MHD mode (MHD- $n1$). The appearance of the initial event says that the plasma will end in a disruption. A detailed explanation of the disruption event chain shown at the top of Fig. 1 can be found in Ref. 1. The DECAF disruption event chain analysis (DIS event in the event chain, marked by a green X in the figure) finds that the start of the event chain appears in the region indicated by the green circle on the disruptivity plot (lower left frame). This region exhibits very low disruptivity. DECAF event characterization and event chain analysis shows that disruption forecasting analysis often starts during plasma operational states and at parameters that appear safe. This fact is completely missed by “disruption database” studies that only process data near the disruption time. This shows that the DECAF analysis makes an early forecast of the disruption (here 77ms earlier than DIS) which is on a transport timescale. Therefore, this forecast would be early enough to trigger actuators purposed to alter the MHD mode state for disruption avoidance, such as systems to change the mode rotation (e.g. neutral beam injection (NBI), or mode entrainment system) or provide MHD mode stabilization. DECAF also computes a continuous warning level (lower right frame) based on 15 different criteria including the frequency evolution of Fourier decomposed MHD mode “objects” (upper right frame), plasma rotation profile, and proximity to the computed mode rotation bifurcation point (loss of torque balance) for the purpose of disruption avoidance.

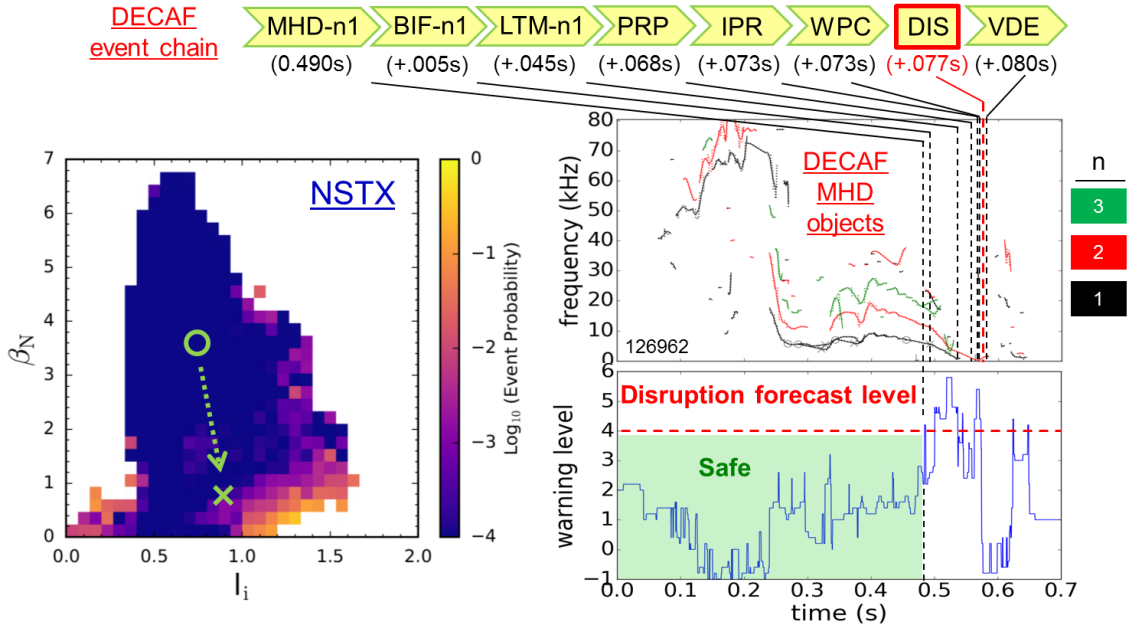


Fig. 1: DECAF disruption event chain analysis and early disruption warning, showing that the event leading the chain occurred when (I_i, β_N) would indicate very low disruptivity.

The DECAF MHD event warning model was applied to the KSTAR device to determine the applicability of the approach to a tokamak with significantly greater aspect ratio $A = 3.5$ compared to NSTX ($A = 1.3$). Fig. 2 shows analysis of a KSTAR plasma with MHD activity that ends in a mode lock and subsequent plasma disruption. Fig. 2a shows the DECAF MHD object decomposition which discretizes a magnetic spectrogram utilizing 14 toroidal magnetic probes. The dominant $n = 1$ mode activity starting at $t = 2$ s eventually leads to the mode lock and the subsequent DECAF disruption warning is shown in Fig. 2b to occur 0.3s before the time of the disruption. This early warning would provide ample time for disruption avoidance to be activated and is also 10 times the suggested minimum warning time to activate disruption mitigation in ITER. Fig. 2c shows a heat map for the conditions used in the determination of the MHD warning level. The warning level is relatively high near $t = 0.7$ s which can be seen is due to the individual warning conditions related to the plasma rotation profile (speed, and its rate of change at different radial positions), decreasing normalized beta, mode frequency,

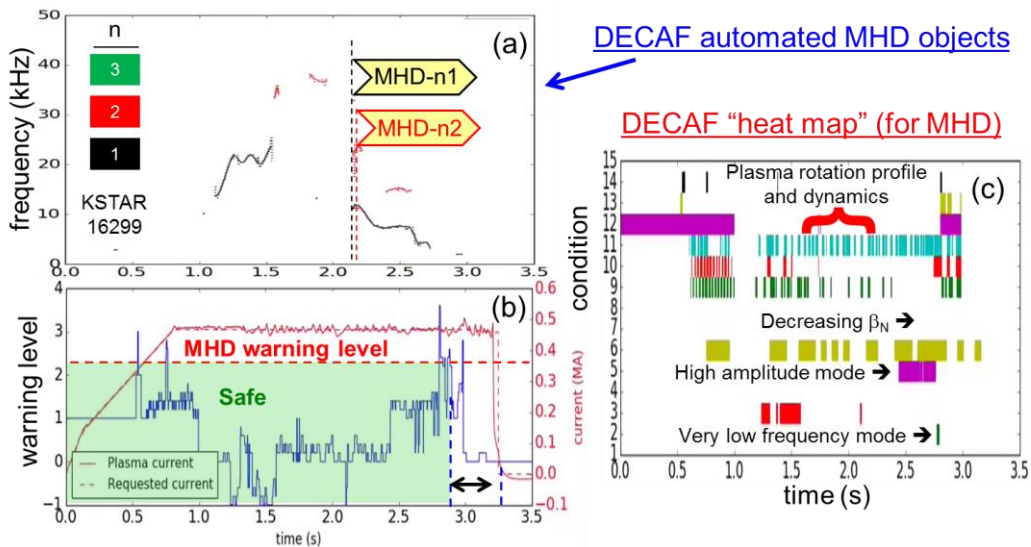


Fig. 2: (a) DECAF MHD object decomposition, (b) DECAF MHD warning level and plasma current evolution, and (c) DECAF heat map of criteria used to determine warning level for a KSTAR plasma mode lock disruption.

rate of change and strength. These individual warnings are seen to not be met by $t = 1.1$ s and the warning level decreases substantially, even though $n = 1$ rotating mode activity exists. The combination of plasma rotation profile and behavior, decreasing β_N , high $n = 1$ mode amplitude and low mode rotation frequency eventually drive the MHD warning to the critical level.

2.2. Disruption prediction performance

Disruption prediction research using DECAF also allows quantifiable figures of merit (i.e. the plasma disruptivity) to provide an objective assessment of the relative performance of different models. This allows an assessment of how well the predictor performs compared to ITER needs. Figure 1 shows a progression of DECAF disruption forecasting models. The earliest models included about 10 events and were run on databases for which the events that led to the disruption were known and yielded very high performance (e.g. 100% true positives). A next evaluation of models focused on earlier forecasting once the first physics forecasting model was implemented in the code. True positives were found to be $\sim 84\%$, which was a measure mainly of a single forecasting model. Forecasting models continue to be added to improve that performance. The next code testing was on large databases $\sim 10,000$ shot*seconds of plasma run time tested (Fig. 3). This was done with a smaller number of events due to computer limitations. With 5 events, applied to all plasma shots from an NSTX database, DECAF shows performance levels of over 91% true positive disruption predictions. False positives in this analysis reached 8.7% which is fairly high. Present code development that allows the events to poll each other will aim to improve the false positive tally.

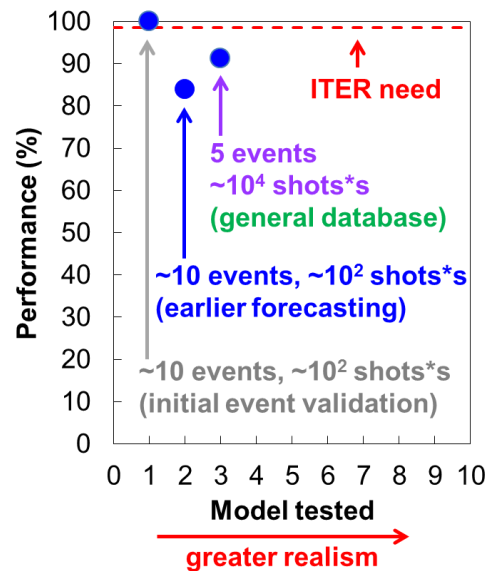


Fig. 3: DECAF model performance evolution (true positive disruption forecast).

2.3. DECAF disruption chain event development

The DECAF code was designed to ease the continued analysis of continuous operation and off-normal event modeling of multiple tokamaks to provide improved understanding of the chains of physical events that lead to a disruption, and to improve disruption prediction and forecasting performance. The code directly integrates the control of real-time algorithms and “offline” (not performed in real-time) analysis. This avoids significant issues in algorithm development related to independent development of real-time implementation from offline analysis. DECAF events also continue to be developed to provide earlier forecasting of the physical phenomena targeted. A few of the latest events include a more rapid analysis and forecasting of locked tearing modes (LTM), ELM identification (ELM), and L-H mode confinement state identification and transitions (HLB). The reduced version of LTM uses a subset (as low as two) toroidally separated magnetic pickup loops and magnetic diagnostics suited for low frequency magnetic perturbation measurements (e.g. partial saddle loops). As low as

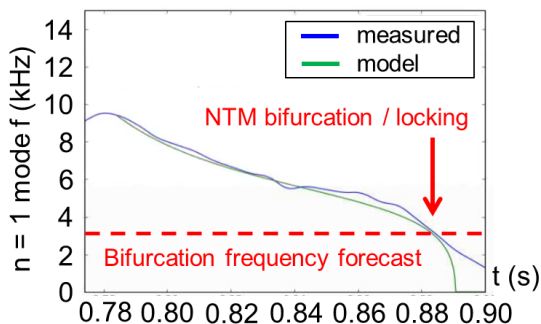


Fig. 4: NTM bifurcation frequency forecasting for the avoidance of locked mode-induced disruptions.

5 warning criteria have been found adequate to produce a usable LTM warning level in offline analysis. However, fast Fourier transform analysis using a larger array of magnetic pickup loops leading to mode decomposition as shown in Fig. 1b and Fig. 2a is presently found to be more accurate. Real-time data acquisition has been installed in KSTAR for this purpose (Section 4) so that the performance of both approaches can be compared in real-time. Fig. 4 shows an example of the locked mode forecasting algorithm under development (applied to an NSTX plasma here). The forecaster presently uses a torque balance model for the rotating magnetic island

following the classic Fitzpatrick model [7] utilizing the equation

$$\frac{d(I\Omega)}{dt} = T_{aux} - \frac{k_2\Omega}{1+k_1\Omega^2} - \frac{I\Omega}{\tau_{2D}} \quad (1)$$

where Ω is the mode rotation frequency, I is the moment of inertia of the plasma in the annular region of the magnetic island, T_{aux} is the torque input by auxiliary sources, and τ_{2D} is the momentum diffusion time of the annular island region. At present, k_1 and k_2 are coefficients representing the strength of resonant and non-resonant drag sources on the mode. Initial analysis has assumed that the plasma in the region of the magnetic island cannot slip relative to the mode, and that resonant drag dominates ($k_1 \gg k_2$; $k_1\Omega^2 \gg 1$). The values T_{aux} , τ_{2D} , and k_1 can be determined in several ways including using further physics modeling or empirically based on existing disruption-free plasma data. If the rotating mode continues to slow, eventually T_{aux} will be insufficient to allow Equation 1 to have a real solution and Ω will rapidly decrease. This critical bifurcation point can be forecast offline or in real-time using Equation 1. Both the modeled mode rotation frequency and the forecast for the bifurcation frequency are shown in Fig. 4. The bifurcation point at $t = 0.88$ s is modeled well and forecast about 80 ms earlier. Results to date show that while the Fitzpatrick model is useful for this forecast, the bifurcation point is sensitive, as expected, to k_1 . This variable is also expected to change during the plasma evolution based on other relevant plasma parameters including the island width. Analysis continues to expand the physics of Equation 1 to further increase the forecast reliability of the bifurcation frequency.

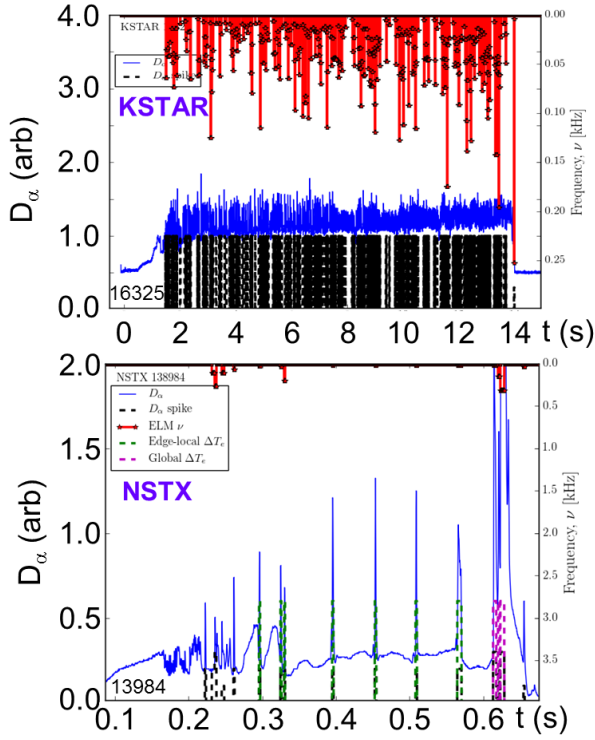


Fig. 5: DECAF ELM detection in KSTAR and NSTX. Blue solid lines show D_α emission and black dashed lines show automated ELM detection. Green dashes indicate that the perturbation is edge-localized and magenta dashes show that perturbation is global.

Automated ELM detection and classification [8] is gathering more attention for real-time analysis by researchers. Since most ELMs do not lead to plasma disruptions tokamaks, the purpose for ELM detection in DECAF is quite different than in other studies. First, ELMs are known to trigger other MHD modes, such as tearing instabilities, that can subsequently lead to disruptions [5]. Second, and also very important, is that transient behavior in D_α emission, usually thought to always represent ELMing in H-mode conditions, need not represent ELMing at all. Transient bursts of D_α emission can, for example, be due to the non-linear evolution of more global MHD activity, which cause minor disruptions (large thermal quenches) which are important to distinguish for DECAF analysis. One reason for this is the potential reduction of false positives in DECAF events. Third, ELMs occur in different ways across devices, and so their comparison across devices is potentially of high value in understanding their role as triggers for disruption-inducing events. Fig. 5 shows ELM detection in DECAF for shots from KSTAR and NSTX. The former illustrates the capability for long pulse plasmas that will be used next to determine the correlation of ELMing and details of tearing mode triggering using the DECAF MHD

event (e.g. shown in Fig. 2a) to determine correlations between the events, and any alterations to either of the events when they occur in close time proximity. The latter illustrates the present DECAF ELM event capability to determine which D_α bursts are *not* indications of ELMs. This is shown, for example, by the magenta dashed lines in the NSTX case near $t = 0.6$ s. Here, Thomson scattering T_e profiles are used to determine the local/global nature of the mode. In KSTAR, this capability will be possible in real time in the near future when real-time electron cyclotron emission data acquisition is activated for KSTAR (Section 4).

3. EXPANDED PHYSICS ANALYSIS SUPPORTING DISRUPTION EVENT CHARACTERIZATION AND FORECASTING

There is an extensive physics research effort supporting DECAF model development. Two research efforts are summarized in this section – resistive wall mode instability studies on MAST and transport analysis of high performance KSTAR plasmas with high non-inductive current fraction. Resistive stability including Δ' calculation by the Resistive DCON code is evaluated for these plasmas using kinetic equilibrium reconstructions with magnetic field pitch angle data to determine the capability for instability forecasting with details given in a separate presentation at this conference by Y. Jiang, *et al.* (Reference [4]).

3.1 Resistive wall instability in MAST

New analysis of MAST plasmas has uncovered global MHD events at high β_N identified as resistive wall modes (RWMs). A stability analysis of MAST plasmas shows a significant ballooning shape of the three-dimensional RWM eigenfunction that compares well to fast camera images (Fig. 7). The MAST RWM eigenfunction shape

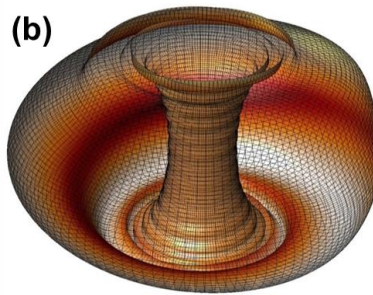
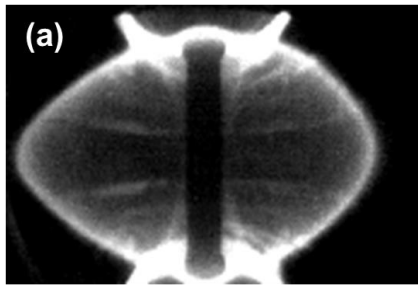


Fig. 7: (a) fast camera image of MAST plasma (21436, $t \sim 0.28s$) displaying an RWM and (b) theoretically computed $n = 1$ RWM eigenfunction of unstable plasma 7090

and growth rate appear significantly altered by the location of conducting structure compared to results from NSTX, which shows a much more spherical shape due to close-fitting copper plates. [9] The conducting wall stabilizing effect on the kink mode is computed to be relatively small in MAST, also in contrast to NSTX that has $\frac{3}{4}$ " thick copper

stabilizing plates. [10] The MAST plasma with an unstable RWM has a computed no-wall β_N limit of 5.0 and a with-wall limit of 5.16 (Fig. 6). The NSTX analysis shown in Ref. 10 shows a kink stabilization range of $5.1 < \beta_N < 6.9$. Another new result of the present MAST analysis shows that kink mode stabilization was primarily due to the vacuum vessel, rather than the conductive shaping coil casings. In contrast to MAST, design equilibria of MAST-U plasmas show a significant increase in kink mode stabilization due to the addition of stainless steel divertor plates. The VALEN RWM stability analysis (Fig. 6) including 3D conducting structure shows a significantly increased kink-stabilized

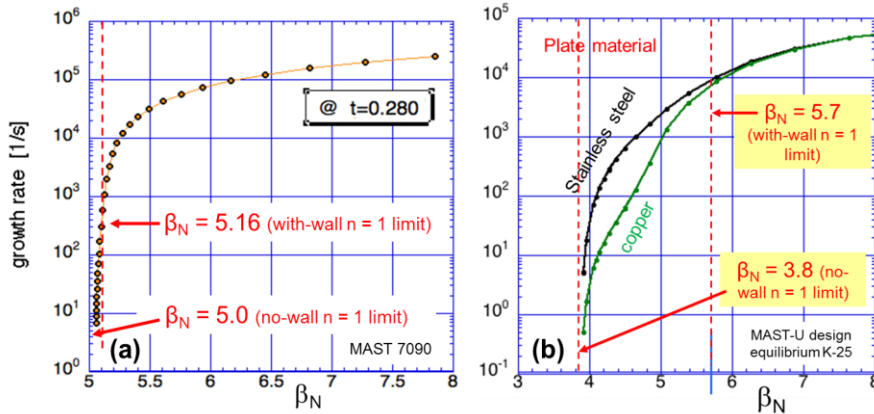


Fig. 6: VALEN RWM growth rate analysis of (a) MAST (less conducting structure) and (b) MAST-U (greater conducting structure, especially in the divertor region).

range ($3.8 < \beta_N < 5.7$). MAST-U design equilibria with closer plasma-plate coupling show a significantly higher with-wall β_N limit. Further analysis detail of MAST-U stability projections can be found in Reference 11.

3.2 Interpretive and predictive transport analysis of high non-inductive current plasmas in KSTAR

To run continuously, a tokamak requires 100% non-inductive plasma current, which can be provided by a combination of plasma-created “bootstrap” current and auxiliary-generated current. Operating continuously 100% non-inductively driven current may pose special challenges for disruption avoidance since this operation will largely, or entirely eliminate inductive current drive which presently provides a key actuator to help

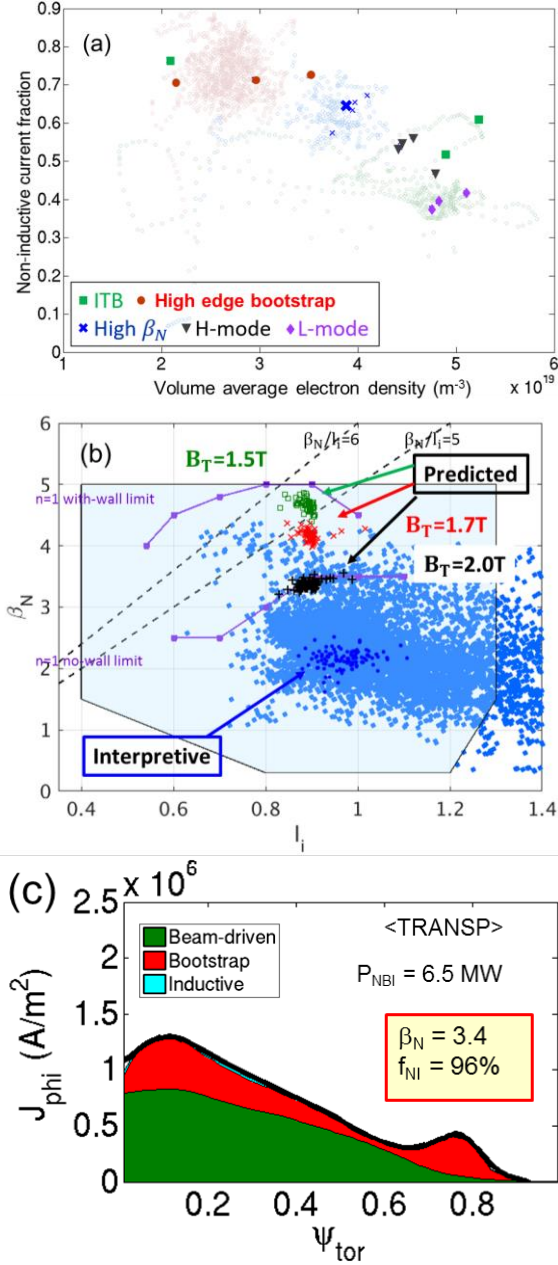


Fig. 8: (a) Computed non-inductive current fraction in present KSTAR operational regimes, (b) operational space (I_i, β_N) of interpretive and predictive TRANSP analysis for 100% non-inductive current fraction scenarios, (c) toroidal current density profile components $\sim 100\%$ NICD plasma.

detect and decompose rotating MHD activity in the device. Fourteen channels (maximum 16) of a toroidal array of magnetic pickup probes have been acquired in real-time during rotating MHD activity. Offline DECAF analysis of the real-time signals shows that the mode decomposition and DECAF object decomposition (same analysis used in Fig. 2a) replicates the local KSTAR spectrogram analysis (Fig. 9). The real-time data acquisition computer hardware includes a field-programmable gate array chip to allow the computation of FFTs used for mode decomposition in real time. Real time software is being written to generate the DECAF MHD object decomposition in real time, which will enable an emulation of the offline DECAF MHD and full LTM event calculations (see Section 2) in real-time. The second example is data from the real-time toroidal plasma velocity system. Data from up to 32 channels at different radial positions on the plasma midplane were gathered. The real-time velocity system (RTV) was tested by validating results against the offline charge exchange recombination spectroscopy system (CER). The RTV system was tested processing 16 channels at 1 KHz and

maintain plasma stability during transient current events that can occur in high performance tokamak plasmas. Therefore dedicated experiments need to be performed to produce such databases for disruption prediction and avoidance research. TRANSP analysis of plasmas created in high performance KSTAR operational regimes shows that the non-inductive current fraction has reached 75% (Fig. 8a). To design experiments to access the fully non-inductive operational regime, “predict-first” TRANSP analysis was performed showing that with the newly-installed 2nd NBI system (assuming usual energy confinement quality and Greenwald density fraction), 100% non-inductive plasmas scenarios are found in the range $\beta_N = 3.5-5.0$ by altering plasma current and toroidal field. (Fig. 8b). The components of the toroidal current density profile are shown in Fig. 8c extrapolated from a KSTAR H-mode operational regime with high edge bootstrap current. When operated, these plasmas will provide a unique long pulse ($\sim 20s$) database for disruption forecasting studies.

4. REAL-TIME EXTENSION OF DISRUPTION EVENT CHARACTERIZATION AND FORECASTING

Real-time DECAF analysis is now being constructed for KSTAR, which required the design, procurement, and installation of significant data acquisition hardware. Four of five real-time (r/t) computers and diagnostic interfaces have been installed to measure and decompose rotating MHD activity, measure the r/t toroidal plasma velocity profile, r/t plasma electron temperature profile, and provide r/t two-dimensional measurement of electron temperature fluctuations at a given toroidal position. A fifth system to provide r/t measurement of the internal magnetic field pitch angle profile using the motional Stark effect is under design for installation in the coming year.

Two examples of data acquired in real time by these systems are shown here. The first has been installed to

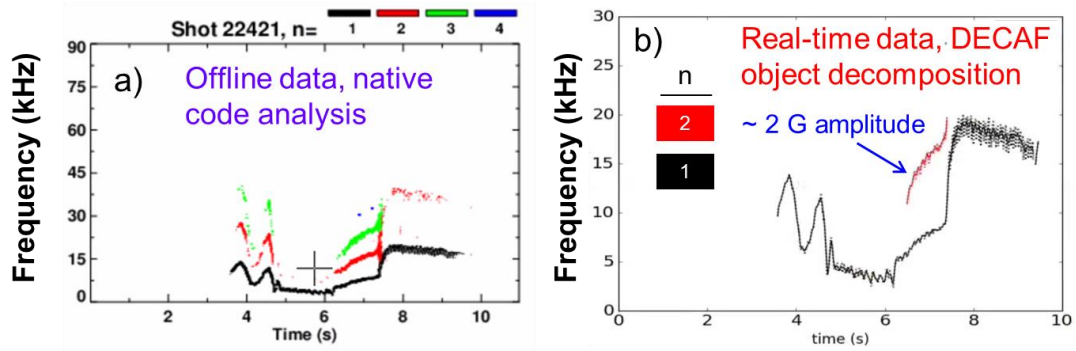


Fig. 9: a) native magnetic spectrogram analysis compared to b) DECAF MHD object decomposition of real-time data (analyzed offline) for KSTAR plasma.

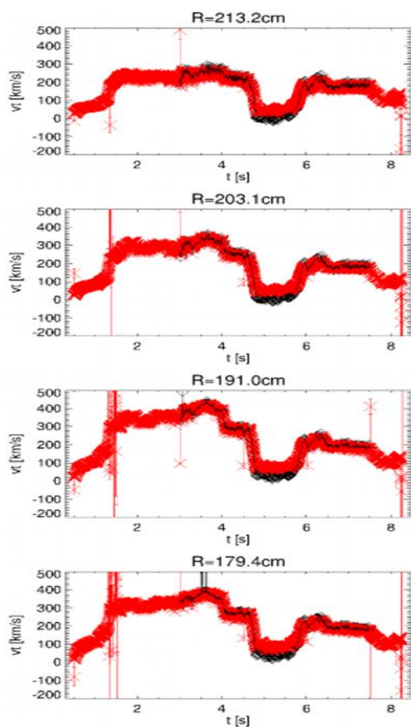


Fig. 10: Comparison of plasma toroidal velocity profile measured by RTV (red) and CES (black) systems on KSTAR.

compared to the equivalent CER channels analyzed at 100 Hz. Fig. 10 shows a comparison of four such channels. In this illustration, the data was acquired in real-time and processed off-line, programmed to attempt replication of the expected real-time analysis scheme. No Ne glow wavelength calibration was performed. A raw calibration was made based on passive spectra and refined through comparison with the CER system. As shown, there is overall good agreement between the toroidal velocity measured by the two systems. The remaining 12 channels show similar good agreement.

Real-time data acquisition from the electron cyclotron emission (ECE) and 2-D ECE imaging systems (ECEI) to measure the T_e profile and 2-D T_e fluctuations is planned to the coming run campaign providing the first such r/t data for r/t DECAF testing.

ACKNOWLEDGEMENTS

This research was supported by the U.S. Department of Energy under contracts DE-SC0016614, DE-SC0018623, and DE-FG02-99ER54524.

REFERENCES

- [1] SABBAGH, S.A., BERKERY, J.W., PARK, Y.S., *et al.*, “Disruption Event Characterization and Forecasting in Tokamaks”, IAEA Fusion Energy Conference 2018 (Gandhinagar, India), paper EX/P6-26.
- [2] HUMPHREYS, D., AMBROSINO, G., DEVRIES, P., *et al.*, Phys. Plasmas **22** (2015) 021806.
- [3] BERKERY, J.W., SABBAGH, S.A., BIALEK, J.M., *et al.*, “Exploration of the equilibrium and stability properties of spherical tokamaks and projection for MAST-U”, submitted to this conference.
- [4] JIANG, Y., SABBAGH, S.A., PARK, Y.S., “Kinetic equilibrium reconstruction and stability analysis of KSTAR plasmas supporting disruption event characterization and forecasting”, submitted to this conference.
- [5] PARK, Y.S., SABBAGH, S.A., JIANG, Y., “Stability of neoclassical tearing modes and their active stabilization in KSTAR”, submitted to this conference.
- [6] DEVRIES, P.C, JOHNSON, M.F., ALPER, B., *et al.*, Nuclear Fusion **51** (2011) 053018.
- [7] FITZPATRICK, R., Nucl. Fusion **33** (1993) 1049.
- [8] SMITH, D., FONCK, R.J., MCKEE, G.R., *et al.*, Plasma Phys. Control. Fusion **58** (2016) 045003.
- [9] SABBAGH, S.A., BERKERY, J.W., BELL, R.E., *et al.*, Nuclear Fusion **46** (2006) 635.
- [10] SABBAGH, S.A., BIALEK, J.M., BELL, R.E., *et al.*, Nuclear Fusion **44** (2004) 560.
- [11] BERKERY, J.W, XIA, G., SABBAGH, S.A., *et al.*, Plasma Phys. Control. Fusion **62** (2020) 085007.